7764 *Biochemistry* **2009,** *48,* 7764–7775
DOI: 10.1021/bi901065t

BIOCHEMISTRY
including biophysical chemistry & molecular biology
Article

Elucidating the Formation of 6-Deoxyheptose: Biochemical Characterization of the GDP-D-*glycero*-D-*manno*-heptose C6 Dehydratase, DmhA, and Its Associated C4 Reductase, DmhB[†]

Frank D. Butty,[‡] Monique Aucoin,[‡] Leslie Morrison,[‡] Nathan Ho,[‡] Gary Shaw,[§] and Carole Creuzenet*[,‡]

[‡]*Department of Microbiology and Immunology, Infectious Diseases Research Group and* [§]*Department of Biochemistry, University of Western Ontario, London, Ontario N6A 5C1, Canada*

Received June 23, 2009; Revised Manuscript Received July 17, 2009

ABSTRACT: 6-Deoxyheptose is found within the surface polysaccharides of several bacterial pathogens. In *Yersinia pseudotuberculosis*, it is important for the barrier function of the O-antigen *in vitro* and for bacterial dissemination *in vivo*. The putative C6 dehydratase DmhA and C4 reductase DmhB, that were identified as responsible for 6-deoxyheptose synthesis based on genetics data, represent potential therapeutical targets. Their detailed biochemical characterization is presented herein. The substrate, GDP-D-*glycero*-D-*manno*-heptose, was synthesized enzymatically from sedoheptulose 7-phosphate using overexpressed and purified GmhA/B/C/D enzymes from *Aneurinibacillus thermoaerophilus*. Overexpressed and purified DmhA used this substrate with high efficiency, as indicated by its K_m of 0.23 mM and k_{cat} of 1.1 s^{-1}. The mass spectrometry (MS) analysis of the reaction product was consistent with a C6 dehydration reaction. DmhB could readily reduce this compound in the presence of NAD(P)H to produce GDP-6-deoxy-D-*manno*-heptose, as indicated by MS and NMR analyses. DmhA also used GDP-mannose as a substrate with a K_m of 0.32 mM and a k_{cat} of 0.25 min^{-1}. This kinetic analysis indicates that although the K_m values for GDP-mannose and GDP-*manno*-heptose were similar, the genuine substrate for DmhA is GDP-*manno*-heptose. DmhB was also able to reduce the GDP-4-keto-6-deoxymannose produced by DmhA, although with poor efficiency and exclusively in the presence of NADPH. This study is the first complete biochemical characterization of the 6-deoxyheptose biosynthesis pathway. Also, it allows the screening for inhibitors, the elucidation of substrate specificity determinants, and the synthesis of carbohydrate antigens of therapeutic relevance.

6-Deoxyheptose has been found so far within the surface polysaccharides of several pathogens including *Yersinia pseudotuberculosis*, *Campylobacter jejuni*, and *Burkholderia* species (*1*−*8*). The modified heptose is present as part of the lipopolysaccharide (LPS)[1] or of the capsule. Although its role on bacterial virulence is not known in most cases, a recent study has demonstrated that 6-deoxyheptose was important for the barrier function of the *Y. pseudotuberculosis* O-antigen against a variety of components of the innate immune system *in vitro* (*9*). It was also important for dissemination of the bacteria to deep organs in a mouse model of infection, although it was not important for colonization (*9*). This validated the genes and enzymes responsible for the biosynthesis of 6-deoxyheptose as antimicrobial targets.

The 6-deoxyheptose biosynthesis pathway (Figure 1) previously proposed (*10*) based on genomic analyses and LPS structural data (*1*, *3*) has been recently confirmed via genetics and via in-depth structural characterization of the LPS of biosynthetic mutants (*9*, *11*). This pathway involves sequentially the putative GDP-D-*glycero*-D-*manno*-heptose C6 dehydratase DmhA and the putative reductase DmhB (Figure 1B). However, both enzymes await biochemical characterization to prove this pathway experimentally and to allow for the screening or design of inhibitors with potential therapeutic value. Deciphering this pathway will eventually allow the synthesis of GDP-6-deoxy-*manno*-heptose and of its derivatives. Such modified heptoses are not commercially available in their sugar nucleotide activated form, which impedes progress in glycobiology, at both the fundamental and applied levels. Indeed, these molecules could be used for the enzymatic biosynthesis of complex carbohydrate epitopes found in various pathogens and that could serve as antigens for vaccination purposes. Also, elucidating the 6-deoxyheptose biosynthesis pathway will facilitate the understanding of the biosynthesis of modified heptoses present in other pathogens.

[†]This work was funded through operating grants from the Natural Sciences and Engineering Research Council (NSERC) of Canada (to C. C.) and the Canadian Institutes of Health Research (to G.S.). C.C. was the recipient of a University Faculty Award from NSERC. L.M. was the recipient of an NSERC USRA studentship. G.S. is a Canada Research Chair in Structural Neurobiology.

*To whom correspondence should be addressed. E-mail: ccreuzen@uwo.ca. Phone: (519) 661-3204. Fax: (519) 661-3499.

[1]Abbreviations: BTP, Bis-Tris-propane; CE, capillary electrophoresis; CHCA, α-cyano-4-hydroxycinnamic acid; DQ-COSY, double quantum filtered correlation spectroscopy; DSS, sodium 4,4-dimethyl-4-silapentane-1-sulfonate; EDTA, ethylenediaminetetraacetic acid; ESI-MS, electrospray ionization mass spectrometry; FPLC, fast-performance liquid chromatography; GDP, guanosine diphosphate; GST, glutathione *S*-transferase; HPLC, high-performance liquid chromatography; HSQC, heteronuclear single-quantum coherence; ITPG, isopropyl β-D-1-thiogalactopyranoside; LPS, lipopolysaccharide; MALDI, matrix-assisted laser desorption ionization; MS, mass spectrometry; NAD(P), nicotinamide adenine dinucleotide (phosphate); NAD(P)H, reduced form of NAD(P); NMR, nuclear magnetic resonance; PCR, polymerase chain reaction; ROESY, rotating-frame NOE spectroscopy; SDS−PAGE, sodium dodecyl sulfate−polyacrylamide gel electrophoresis; TEAB, triethylammonium bicarbonate; TOCSY, total correlation spectroscopy; Tris, tris(hydroxymethyl)aminomethane; WET, water suppression enhanced through T_1 effects.

 Published on Web 07/17/2009

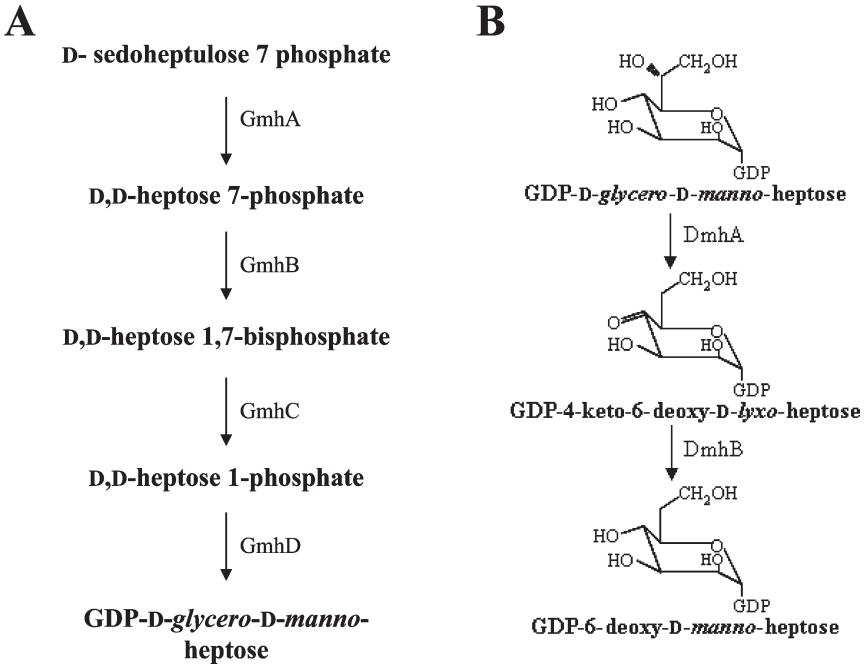

FIGURE 1: Biosynthetic pathways leading to the production of GDP-6-deoxy-*manno*-heptose from sedoheptulose phosphate. Panel A: Biosynthetic pathway showing the four successive enzymatic reactions catalyzed by GmhA/B/C/D, allowing the conversion of D-sedoheptulose 7-phosphate into GDP-*manno*-heptose. Panel B: The two-step pathway that allows conversion of GDP-*manno*-heptose into GDP-6-deoxy-*manno*-heptose via action of DmhA and DmhB (*13*).

As mentioned above, the lack of a commercially available nucleotide-activated heptose-based substrate is a problem for glycobiology and has rendered the biochemical characterization of DmhA and DmhB very difficult. The chemical synthesis of the putative substrate GDP-D-*glycero*-D-*manno*-heptose (referred to as GDP-*manno*-heptose thereafter) was described earlier (*12*), but it cannot be implemented easily on a large scale outside of specialized chemistry laboratories. A four-step enzymatic pathway leading to GDP-*manno*-heptose starting from sedoheptulose 7-phosphate was recently described (Figure 1A) (*13*).

In this report, the four enzymes mentioned above were used to generate a stock of GDP-*manno*-heptose suitable for the enzymatic characterization of DmhA and DmhB, which was done using mostly capillary electrophoresis (CE), mass spectrometry (MS), and NMR. We investigated the GDP-*manno*-heptose C6 dehydratase activity of DmhA and the C4 reductase activity of DmhB, determined the optimal reaction conditions, and analyzed the reaction products by MS and NMR. We also investigated the ability of DmhA and DmhB to use GDP-mannose and its 4-keto-6-deoxy derivative as substrates. To our knowledge, this is the first biochemical characterization of a GDP-*manno*-heptose C6 dehydratase and its associated reductase. The data obtained open the way to screening of inhibitors, for the analysis of other putative heptose dehydratases, and for the elucidation of substrate specificity determinants via structure/function studies.

MATERIALS AND METHODS

Preparation of Expression Constructs for GmhA, GmhB, GmhC, and GmhD. Plasmids containing the *gmhA*, *gmhB*, *gmhC*, and *gmhD* genes from *Aneurinibacillus thermoaerophilus* cloned into the Gateway pDONR201 vector (Invitrogen) were kindly provided by Dr. Messner (Vienna, Austria) (*13*, *14*). The *gmhA*, *gmhB*, and *gmhC* genes were transferred into the pDEST17 vector (Invitrogen) to allow protein expression as N-terminally histidine-tagged proteins. The *gmhD* gene was transferred into pDEST15 to allow the expression of GmhD as a N-terminally glutathione *S*-transferase (GST) tagged protein. The transfer to the pDEST vectors was performed following the Gateway procedure (Invitrogen) as recommended by the manufacturer, using *Escherichia coli* Novablue and ampicillin selection (100 μg/mL). The clones were screened by restriction digestion using *Eco*RI, by PCR using T7 promoter and T7 terminator primers, and finally by DNA sequencing. The sequencing was performed at the Robarts Institute Sequencing Facility (London, Canada).

Cloning of dmhA and dmhB in the pET Vector. The *dmhA* and *dmhB* genes from *Y. pseudotuberculosis* O:2a were PCR amplified from pUC-dmhB/A (*9*) using the primers YPDMHA P4 (AGGGTCCATGGGCATGAATAATGTTTTAATTACAGGT) and YPDMHAP5 (GCGACGGATCCTTAGCGATTTAATGGAATGCG) for *dmhA* and YPDMHB P4 (AGGGTCCATGGGCATGACAAAGGTGTTTATATTAGG) and YPDMHB P5 (GCGTCGGATCCTTATTCCTTAATTACTTCCAGATATGG) for *dmhB*. The PCR was performed using Expand Long Range DNA polymerase (Roche Diagnostics) as recommended by the manufacturer. The PCR products were digested with *Nco*I and *Bam*HI and were cloned into the pET23 derivative (*15*) with an N-terminal histidine tag. The constructs were transformed into *E. coli* JM109 with ampicillin selection (100 μg/mL). The resulting plasmids pET-*dmhA* and pET-*dmhB* were then purified using the GFX kit (GE-Healthcare) and verified by DNA sequencing.

Cloning of HP0044 as a GST-Tagged Protein. HP0044 is a previously characterized GDP-mannose dehydratase from *Helicobacter pylori* that was used as a control in this study. The gene for HP0044 was PCR amplified from chromosomal DNA from *H. pylori* strain 26695, using primers HP0044 P1 (ATGTCAGCTTGAATCAAAC) and HP0044 P2 (GCGTCGGATCCTCATTCATAAAAATTCCTTA). The PCR was done

using Expand Long Range DNA polymerase. The PCR product was cleaved with *Bam*HI and *Eco*RV and cloned into the vector pBluescript SK that had been cut with the same enzymes. The gene was then subcloned into the vector pGEX-2T by PCR using primers HP0044 P5 (AAGACGGATCCATGAAAGAAAAA-ATCGCTTTAATCAC) and HP0044 P6 (GCCTCGAATTCT-CATTCATAAA AATTCCTTAAAATATAAC) and digestion with *Bam*HI and *Eco*RI. After transformation into *E. coli* DH5α and ampicillin selection (100 μg/mL), the plasmid was extracted and sequenced.

Protein Expression and Purification. For all proteins except HP0044, protein expression was performed in *E. coli* BL21(DE3)pLys, using Luria−Bertani broth (LB) or media I, II, or III supplemented with 100 μg/mL ampicillin and 34 μg/mL chloramphenicol. Media I contained 0.6% Na_2HPO_4, 0.3% KH_2PO_4, 0.05% NaCl, 0.1% NH_4Cl, 0.05% $MgSO_4 \cdot 7H_2O$, 0.0015% $CaCl_2$, 0.2% casamino acids, and 0.2% glucose. Media II contained 1% bactotryptone, 0.5% yeast extract, 0.5% NaCl, and 0.2% glucose. Media III contained 2% bactotryptone, 0.2% Na_2HPO_4, 1% KH_2PO_4, 0.8% NaCl, 1.5% yeast extract, and 0.2% glucose (*16*). Protein expression was induced by the addition of 0.15 mM isopropyl β-D-1-thiogalactopyranoside (IPTG). For GmhA, GmhB, and GmhC, expression was carried out in 1 L (for GmhA and GmhC) or 2 L (for GmhB) of LB at 25 °C with 3 h induction. For GmhD, expression was carried out in 2 L of LB at 15 °C or room temperature or in media I, II, or III at room temperature for ∼16 h. For DmhA, overexpression of the protein was performed in LB for 3 h at 37 °C. For DmhB, overexpression of the protein was performed in LB for 18 h at room temperature. For HP0044, protein expression was carried out in DH5α in LB with induction overnight at 30 °C with 0.1 mM IPTG. For all proteins, at the end of the induction period, the cells were harvested by centrifugation (15300*g*) and stored at −20 °C until needed.

To determine whether the proteins were overexpressed in a soluble form, a cell pellet obtained from 1.5 mL of induced culture was treated with 150 μL of 2 mM ethylenediaminetetraacetate (EDTA), 0.1 mg/mL lysozyme, 0.1% Triton X-100, 20000 units of DNase, and 10 mM $MgCl_2$ in 50 mM Tris-HCl, pH 8.0, for 30 min at 30 °C. The soluble proteins were separated from cellular debris and insoluble proteins by centrifugation at 15300*g* for 15 min at 4 °C. The pellets containing the insoluble proteins were resuspended in 50 mM Tris-HCl, pH 8.0, containing 2 mM EDTA. The fractions were run on 10% SDS−PAGE gels and analyzed by Coomassie blue staining or, when applicable, by anti-histidine tag Western blotting using a mouse anti-His IgG antibody (Sigma-Aldrich) and an Alexa Fluor 680 labeled goat anti-mouse IgG antibody (Molecular Probes). Detection was performed using a Li-Cor Odyssey infrared imaging system.

Purification of GmhD and HP0044 by GST Affinity Chromatography. The cell pellet obtained after overexpression of HP0044 or of GmhD was resuspended in 30 mL of PBS binding buffer, pH 8 (140 mM NaCl, 2.7 mM KCl, 10 mM Na_2HPO_4, 1.8 mM KH_2PO_4). Lysozyme was added (150 μg/mL), and the sample was incubated on ice for 15 min before being passed through a French press three times. Cellular debris and insoluble proteins were removed by centrifugation for 20 min at 15300*g* and by filtration through a 0.2 μm filter. GST affinity purification was completed on an FPLC system using a 1 mL GSTrap FF column (GE Healthcare) that had been equilibrated in PBS binding buffer. The protein was loaded twice, and the column was washed with 10 column volumes (CV) of binding buffer. The GmhD protein was eluted with 3 CV of 0.01 M reduced glutathione. The glutathione was removed from the sample by overnight dialysis (cutoff of 3500 Da) in 50 mM Tris-HCl, pH 8, at 4 °C. For HP0044, the GST tag was removed by on-column incubation with thrombin for 2 h at 37 °C, and the protein was eluted in 5 CV of 50 mM Tris-HCl buffer, pH 8. The purified proteins were analyzed by SDS−PAGE and Coomassie staining and were stored in 50% glycerol at −20 °C.

Purification of Histidine-Tagged Proteins (*GmhA, GmhB, GmhC, DmhA, and DmhB*) *by Nickel Chelation*. The induced cell pellets were resuspended in 30 mL of binding buffer, pH 7.5 (20 mM imidazole, 20 mM Tris-HCl, and 0.1 M NaCl). Lysozyme addition, cell lysis, centrifugation and filtering steps were completed as described above. The histidine-tagged proteins were purified by FPLC (Akta purifier) using a 1.6 mL Poros MC 20 column (4.6 mm × 100 mm; Applied Biosystems) that had been loaded with nickel sulfate and equilibrated with 10 CV of binding buffer. The sample was passed through the column twice before the column was washed with 10 CV of binding buffer. The proteins of interest were eluted by a linear gradient of imidazole from a concentration of 50 mM to 1 M in 30 CV. The fractions that contained the pure protein of interest were pooled and dialyzed (cutoff of 3500 Da) in 50 mM Tris-HCl, pH 7.5, overnight at 4 °C. The purified proteins were analyzed by SDS−PAGE as described above, quantitated using the Bio-Rad protein determination reagent and a standard curve of bovine serum albumin following the manufacturer's instructions, and were stored in 50% glycerol at −20 °C.

Preparation of GDP-manno-heptose using GmhA/B/C/D. Sedoheptulose 7-phosphate was obtained from GlycOTeam GmbH (Germany). To monitor the stepwise conversion of sedoheptulose 7-phosphate into GDP-*manno*-heptose 1-phosphate, 30 μL reactions containing 0.5 mM sedoheptulose 7-phosphate, 10 mM $MgCl_2$, and 1 mM ATP in 200 mM Tris-HCl, pH 8, with either no enzyme, GmhA alone, GmhA and GmhB, GmhA, GmhB, and GmhC, or all four enzymes were incubated for 5 h at 37 °C. Approximately 8, 24, 13, and 20 pmol of GmhA, GmhB, GmhC, and GmhD, respectively, were used in each reaction as needed. These reactions were analyzed by HPLC as described below.

A large-scale reaction of 2.5 mL was set up to produce heptose 1-phosphate. It contained 1.25 mM sedoheptulose 7-phosphate, 50 mM $MgCl_2$, 1.3 mM ATP, 1.68 nmol of GmhA, 0.75 nmol of GmhB, and 0.65 nmol of GmhC in 400 mM Tris-HCl, pH 9.0. The reaction was incubated 5 h at 37 °C. This reaction was then used to generate GDP-*manno*-heptose via the addition of GTP to 0.6 mM and 1.44 nmol of GmhD in a final volume of 4 mL. The reaction was incubated further for 5 h at 37 °C. The final conversion into GDP-*manno*-heptose by GmhD was monitored by capillary electrophoresis (CE) with UV detection as described below.

HPLC Analysis of Various Sugars. HPLC analysis was performed on a Dionex ICS 3000 instrument equipped with an electrochemical detector with a gold electrode and used in the integrated amperometric detection mode essentially as reported previously (*13*). The samples were analyzed on a CarboPac PA1 column (4 × 250 mm; Dionex) that had been equilibrated in 100 mM NaOH for 10 min at 1 mL/min. Ten microliters of sample diluted to 0.1 mM in 100 mM NaOH was injected, and a 40 min linear gradient of 100−500 mM NaOAc in 100 mM NaOH was applied at 1 mL/min.

Capillary Electrophoresis of Sugar Nucleotides. CE was performed on a Beckman Gold instrument using the 32 Karat software and a 57 cm bare silica capillary. The initial conditioning of the capillary was performed by washing the capillary with 0.1 N HCl for 30 min at 20 psi, followed by 10 min of water. For sample analyses, the capillary was washed for 2 min with 200 mM borax, pH 9, buffer, the sample was injected by pressure for 4 s, and separation was performed by applying 26 kV to both ends of the capillary that were maintained in the borax buffer. Migrating compounds were monitored at 254 nm in a window placed at 50 cm from the beginning of the capillary. The capillary was washed 2 min with water, 2 min with 0.1 M NaOH, and 2 min again with water between each run. Substrate conversion was estimated by integration of the surface areas under the substrate and product peaks using the 32 Karat software.

Purification of Sugar Nucleotides. All sugar nucleotides were purified by anion-exchange chromatography using a High Q Econopac 1 mL column (Bio-Rad) (*17*) and a linear gradient of 20 column volumes of triethylammonium bicarbonate (TEAB), pH 8.5 (50 mM to 1 M), at 1 mL/min with UV detection (260 and 214 nm). The fractions containing the product of interest were pooled and lyophilized twice with resuspension in water between both lyophilization steps. They were then resuspended in water for assessment of purity by CE and of identity by mass spectrometry (MS) analysis. Quantitation was performed using a Nanodrop spectrophotometer and using $\varepsilon_{GTP} = 12000\ mol^{-1}\ L\ cm^{-1}$.

Enzyme Assays with DmhA, DmhB, and HP0044. Typically, reactions were performed by incubating between 0.1 and 22 pmol of DmhA, HP0044, and/or DmhB with 0.1−0.2 mM substrate (GDP-*manno*-heptose prepared above or commercial GDP-mannose (Sigma)) in 200 mM Tris-HCl buffer, pH 9.5 or 8.5 (as specified in the legends to the figures), in a final volume of 10 μL unless stated otherwise. Cofactors $NAD(P)^+$ and NAD(P)H were added to 0.2 mM, when necessary. The reactions were incubated for as little as 2 min to up to overnight at 37 °C. When appropriate, the buffer was replaced by 200 mM TEAB, pH 8.5. Specifics for each experiment are stated in the legends to the figures. The reaction products were analyzed by CE as described above. Large-scale reactions were prepared by direct proportional increase of all components for anion-exchange purification followed by MS or NMR.

For the temperature study for DmhA, the reactions contained 0.44 pmol of DmhA and 0.1 mM GDP-*manno*-heptose in a total volume of 10 μL of 200 mM Tris-HCl, pH 9. They were incubated for 10 min at temperatures ranging from 4 to 65 °C. For DmhB, a stock reaction containing 4.4 pmol of DmhA, 0.1 mM GDP-*manno*-heptose, and 0.1 mM NADH in a total volume of 100 μL of 200 mM Tris-HCl, pH 9, was incubated for 20 min at 37 °C to ensure 100% conversion into the 4-keto derivative. Then 0.6 pmol of DmhB was added to 7 μL of this reaction stock, the final volume was brought up to 10 μL, and the samples were incubated for 20 min at temperatures ranging from 4 to 65 °C.

For the pH studies, the DmhA reactions contained 0.89 pmol of DmhA and 0.1 mM substrate in a total volume of 10 μL. The reactions were performed in 200 mM NaOAc buffer for pH 5−7 and in 200 mM Bis-Tris-propane (BTP) for pH 7−10.5. They were incubated at 37 °C for 10 min. To determine the pH optimum for DmhB, a stock reaction of 4.4 pmol of DmhA, 0.1 mM GDP-*manno*-heptose, and 0.1 mM NADH in a total volume of 100 μL of 200 mM Tris-HCl, pH 8, was incubated for 20 min at 37 °C to ensure 100% conversion into the 4-keto derivative. Aliquots of 7 μL were withdrawn, and their pH was adjusted to the appropriate value by addition of 1 M Tris-HCl for pH 7−8.0 or BTP for pH 8.0−10.5. Then 0.6 pmol of DmhB was added, the volume was brought to 10 μL, and the samples were incubated for 20 min at 37 °C.

To test for cofactor dependence, $NAD(P)^+$ and NAD(P)H were added to a final concentration of 0.1 mM in DmhA and DmhB reactions, respectively.

For determination of K_m, V_{max}, and turnover parameters, 11 reactions with varying concentrations of substrate (0.1−0.5 mM) were set up in duplicates and incubated for 2 min (for GDP-*manno*-heptose series) or 60 min (for GDP-mannose series) at 37 °C, which ensured less than 10% substrate conversion over the whole range of substrate concentrations tested. The data are the average of two independent experiments and were calculated using the Lineweaver equation. All reactions were flash frozen in a dry ice−ethanol bath and ran individually immediately after thawing.

To decipher whether all reaction products observed in DmhA reactions were the result of enzymatic activity or not, a 70 μL reaction containing 62 pmol of DmhA and 0.1 mM GDP-*manno*-heptose in 200 mM TEAB, pH 8.5, was incubated at 37 °C for 30 min. The reaction was quenched by flash freezing in dry ice−ethanol. The enzyme was then removed by ultrafiltration (Nanosep centrifugal device, 10 kDa cutoff (Pall, Life Sciences)). The filtrate was analyzed by CE. A 10 μL aliquot of the ultrafiltrate was supplemented with 0.1 mM (final concentration) GDP-*manno*-heptose and was further incubated at 37 °C for 30 or 60 min. Also, aliquots (10 μL each) of the ultrafiltrate were further incubated at 37 °C for 30, 45, 60, or 90 min and analyzed by CE. A complete (unfiltered) reaction was also incubated at 37 °C for 60 min and served as a positive control.

Mass Spectrometry Analyses. Mass spectrometry analyses of the sugar nucleotides and cofactors were performed at the Dr. Don Rix Protein Identification Facility of the University of Western Ontario. All sugar nucleotides and cofactors were analyzed by ESI-MS on a Micromass Qtof spectrometer equipped with a Z-spray source operating in the negative ion mode (40 V, 80 °C). Calibration was performed with NaI, and acquisition was performed using the software MassLynx 4.0 (Micromass). GDP-*manno*-heptose and products P2 and P2′ were purified by anion-exchange chromatography before analysis. The DmhA reaction product (product P1) was analyzed similarly except that, due to its instability, it was generated directly in TEAB buffer (100 mM, pH 8.5), flash frozen, partially lyophilized, and resuspended in ice-cold water twice, before final resuspension in ice-cold water for MS analysis. The sample was maintained frozen or on ice at all times to avoid degradation. The DmhB product (P3) was also produced in TEAB for MS analyses.

To identify the cofactor present within DmhA, 5 nmol of DmhA resuspended in 1 mL of 50 mM ammonium bicarbonate, pH 8, was boiled for 5 min, filtered through an Amicon ultracentrifugation device (3 kDa cutoff), concentrated down to 20 μL by lyophilization, and analyzed by MS as indicated above.

Purified DmhA and DmhB proteins were analyzed by MALDI mass spectrometry using a 4700 Proteomics analyzer (Applied Biosystems, Foster City, CA) in the linear positive ion mode to confirm their size. The MALDI matrix, α-cyano-4-hydroxycinnamic acid (CHCA), was prepared as 5 mg/mL in 6 mM monobasi ammonium phosphatec, 50% acetonitrile, and 0.1%

trifluoroacetic acid and mixed with the sample 1:1 (v/v). Data acquisition and data processing were respectively done using 4000 Series Explorer and Data Explorer (both from Applied Biosystems). The analysis was performed at the MALDI mass spectrometry facility of the University of Western Ontario (London, Ontario, Canada).

NMR Analysis of GDP-manno-heptose and of the DmhB Reaction Product. A 3 mL reaction containing 0.33 mM GDP-*manno*-heptose, 220 pmol of DmhA, 304 pmol of DmhB, and 0.5 mM NADPH in 200 mM TEAB, pH 8.5, was incubated overnight at 30 °C. The reaction progress was assessed by CE. Once the reaction had reached completion, the product was purified by anion-exchange chromatography using a 5 mL High Q Econopac column as described above. The fractions containing the pure product (as assessed by CE) were pooled, lyophilized, resuspended in 350 μL of D_2O, lyophilized again, and resuspended in D_2O twice more before being analyzed by NMR spectroscopy. The final sample (1.7 mM final) was dissolved in 350 μL of D_2O and placed in a 5 mm Shigemi NMR tube having 5 μM DSS as an internal standard. An identical sample of GDP-glycero-*manno*-heptose was prepared for comparison.

All ^{1}H NMR data were collected with a Varian Inova 600 MHz NMR spectrometer at 25 °C. One-dimensional ^{1}H NMR spectra were collected using the WET water suppression sequence. Two-dimensional ^{1}H TOCSY spectra (*18*), using a 5 kHz spinlock and DQ-COSY spectra (*19*), were collected for 256 complex increments. Natural abundance ^{1}H−^{13}C HSQC experiments (*20*, *21*) were also used to confirm all assignments. All spectra were processed using VnmrJ, baseline corrected, and referenced to DSS at 0.00 ppm.

RESULTS

Expression and Purification of the GDP-manno-heptose Biosynthetic Enzymes and Preparation of GDP-manno-heptose. The isomerase GmhA, kinase GmhB, phosphatase GmhC, and pyrophosphorylase GmhD (Figure 1A) were overexpressed in *E. coli* essentially as described before (*13*) and were used for the preparation of GDP-*manno*-heptose. Sedoheptulose 7-phosphate was converted successively into D,D-heptose 7-phosphate, D-α-D-heptose 1,7-bisphosphate, D-α-D-heptose 1-phosphate, and GDP-*manno*-heptose by the consecutive action of GmhA, GmhB, GmhC, and GmhD (*13*) as monitored by anion-exchange chromatography (Figure 2A). The patterns were consistent with those described previously (*13*). However, the presence of the GTP that is necessary to the activity of GmhD inhibited GmhB (Figure 2A, trace e). Consequently, for the large-scale preparation of GDP-*manno*-heptose, heptose 1-phosphate was first prepared using GmhA, GmhB, and GmhC. It was then converted to GDP-*manno*-heptose by the addition of GmhD and GTP. The final reaction was analyzed by capillary electrophoresis (CE) with UV detection of the nucleotide moiety of the final product. A new reaction product not present in control reactions appeared at ~9.5 min on the CE electrophoregram in the presence of GmhD (Figure 2B, traces a and b). This product was purified by anion-exchange chromatography (Figure 2B, trace c) and was analyzed by MS and NMR. Its MS pattern was as expected for GDP-*manno*-heptose as the peak corresponding to the full-size molecule $(M - H)^-$ was observed at m/z 634. Peaks corresponding to expected fragments of the GDP moiety (at m/z 150, 344, 362, 424, and 442) were observed by MS/MS of the parent peak (Figure 3A). Also, a peak corresponding to the

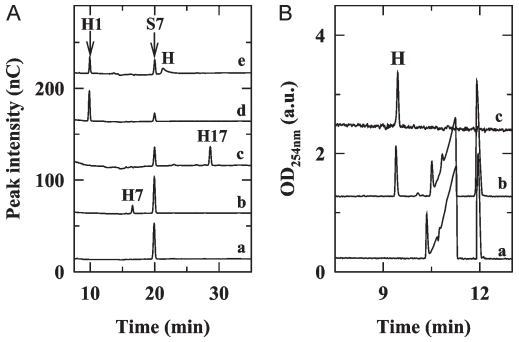

FIGURE 2: Enzymatic preparation of GDP-6-deoxy-*manno*-heptose from sedoheptulose phosphate. Panel A: HPLC chromatograms showing the conversion of sedoheptulose 7-phosphate into GDP-*manno*-heptose by the sequential activity if GmhA, GmhB, GmhC, and GmhD. Traces: a, no enzyme; b, GmhA only; c, GmhA and GmhB; d, GmhA, GmhB, and GmhC; e, all four enzymes. Key: S7, sedoheptulose 7-phosphate; H7, heptose 7-phosphate; H17, heptose 1,7-bisphosphate; H1, heptose 1-phosphate; H, GDP-*manno*-heptose. Panel B: CE electrophoregram showing the conversion of heptose 1-phosphate into GDP-*manno*-heptose (peak H) upon activity of GmhD. Traces: a, no GmhD; b, with GmhD; c, purified reaction product. The peaks present downstream of peak H (between 10.3 and 12.1 min) correspond to leftover nucleotides (ATP, GTP, and derivatives) that were present in excess in the reaction and were eliminated during the purification process.

heptose diphosphate minus one OH group was detected at m/z 351. The NMR pattern was also as anticipated for GDP-*manno*-heptose (Figure 4A and Table 1) as assessed by comparison with previously published data (*13*).

Specifically, the position of the heptose H1 (5.50 ppm) and large coupling constant (7.8 Hz) was indicative of a neighboring phosphate linkage. In addition, complete correlations throughout the heptose ring could be identified in DQ-COSY and TOCSY spectra that provided assignments nearly identical to those previously published for GDP-α-D-α-heptose. Peak integration revealed a 1:1 ratio between the ribose H1 (5.93 ppm) and heptose H1 (5.50 ppm) as expected from the product containing both the ribose and heptose moieties.

Expression and Purification of DmhA and DmhB. DmhA and DmhB from *Y. pseudotuberculosis* O:2a could be overexpressed in *E. coli* BL21(DE3)pLysS at high yield in a soluble form with an N-terminal hexahistidine tag, using the pET system. They were purified to near homogeneity in a single step of nickel chelation affinity chromatography and migrated at the expected size of ~40 kDa for DmhA and ~33 kDa for DmhB (Figure 5). The overexpressed proteins reacted readily with the anti-His antibody, thereby verifying their identity. The enzymes were also analyzed by MALDI MS, and peaks of the expected sizes were obtained at m/z 40100 for DmhA and m/z 33066 for DmhB (data not shown). DmhB was prone to oligomerization, producing a stable dimer that was reactive with the anti-His antibody and was not fully dissociated upon boiling for 5 min in SDS−PAGE sample buffer. DmhB was also prone to heat-induced degradation, producing an ~25 kDa fragment upon processing for SDS−PAGE analysis. This fragment was not present in the original (unheated) sample as per MALDI-MS analysis.

DmhA Uses GDP-manno-heptose as a Substrate. When GDP-*manno*-heptose was incubated with low amounts of DmhA for short periods of time at 37 °C, the formation of a novel product migrating slightly upstream of GDP-*manno*-heptose was observed by CE using UV monitoring of the GDP moiety of the substrate and product (Figure 6A, peak P1). This peak was not

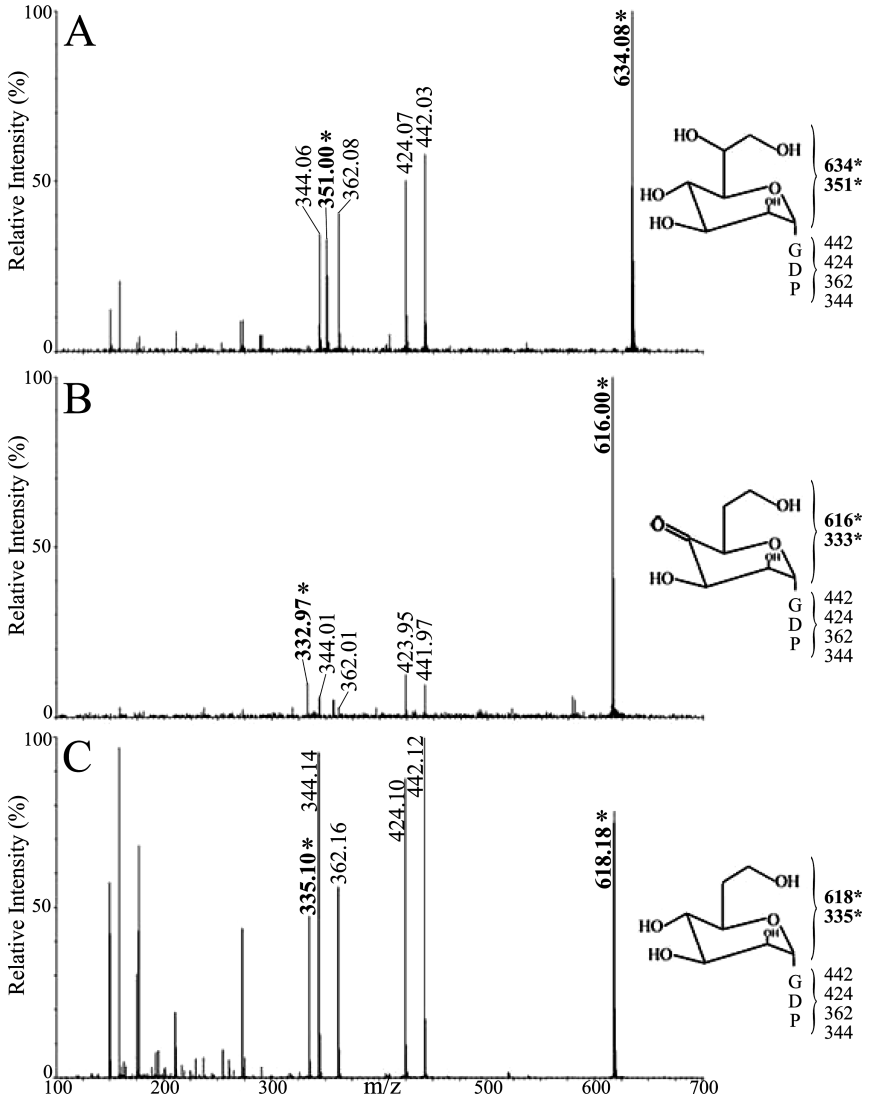

FIGURE 3: Mass spectrometry analysis of the DmhA substrate GDP-*manno*-heptose and of the reaction products P1 and P3. Panel A: MS/MS spectrum of the purified GDP-*manno*-heptose phosphate obtained by conversion of sedoheptulose 7-phosphate by GmhA/B/C/D. This compound was used as a substrate for DmhA throughout this study unless stated otherwise. Panel B: MS/MS spectrum of the reaction product P1 obtained upon incubation of DmhA with GDP-*manno*-heptose. Panel C: MS/MS spectrum of the reaction product P3 obtained upon incubation of DmhB with the DmhA product. For all panels, the structure of the sugar is depicted along with the fractionation pattern that yields peaks present on the MS/MS spectra. Peaks highlighted in bold and with an asterisk indicate peaks comprising the *manno*-heptose ring.

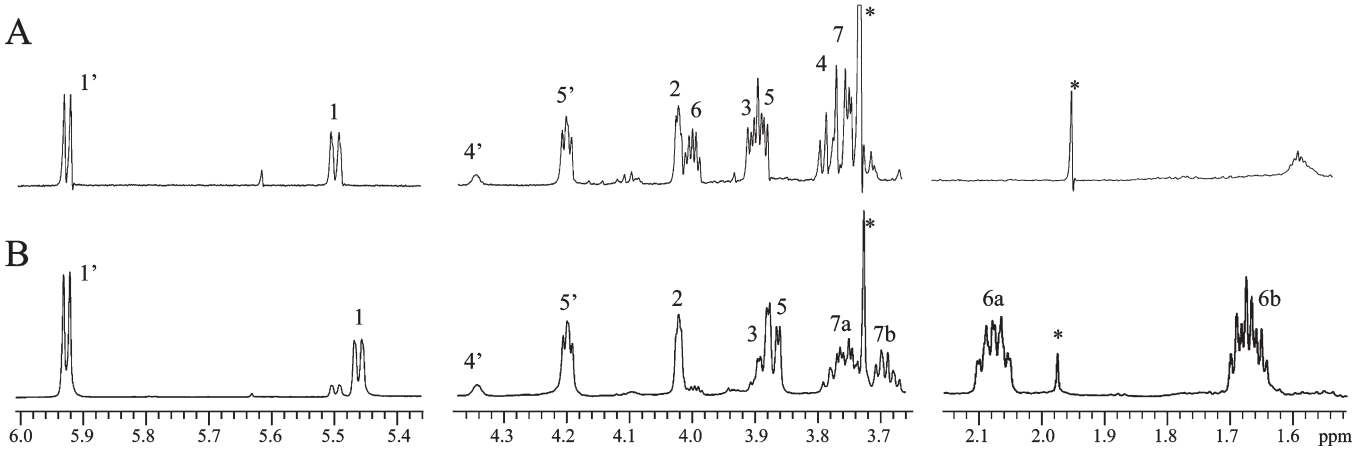

FIGURE 4: NMR analysis of the DmhA substrate GDP-*manno*-heptose and of the DmhB reaction product P3. Panel A: Portions of the 600 MHz ^{1}H NMR spectrum of the purified GDP-*manno*-heptose obtained by conversion of sedoheptulose 7-phosphate by GmhA/B/C/D. Panel B: ^{1}H NMR spectrum of the reaction product P3 obtained upon incubation of DmhB with the DmhA product. Proton H4 from P3 is found at 3.50 ppm and not shown in this figure. Each spectrum shows the assignment of the mannose (1−7) and ribose (1′−5′) protons based on DQ-COSY and TOCSY experiments. In panel B a minor amount of GDP-*manno*-heptose is present. Peaks labeled * result from small buffer impurities. The spectral regions are not scaled identically.

Table 1: ^{1}H NMR Analysis of the GDP-*manno*-heptose Substrate and of the DmhB Reaction Product P3

	H1	H2	H3	H4	H5	H6	H7
GDP-glycero-*manno*-heptose							
^{1}H	5.50	4.02	3.90	3.76	3.88	3.99	3.74
$^{3}J_{HH}$ ($^{3}J_{HP}$)	1.6 (7.8)	2.8	10.3	10.4	3.5		
^{13}C	99.1	72.9	76.6	64.7	72.8	74.9	62.2
ribose							
^{1}H	5.93	4.77	4.52	4.34	4.20		
$^{3}J_{HH}$	6.2						
^{13}C	89.8	76.2	73.3	86.6	68.1		
GDP-deoxy-*manno*-heptose							
^{1}H	5.45	4.03	3.89	3.50	3.87	2.07, 1.67	3.75, 3.69
$^{3}J_{HH}$ ($^{3}J_{HP}$)	1.7 (7.4)	3.0	8.7	9.7		14.6	
^{13}C	99.1	73.0	72.9	73.1	72.9	36.2	60.8
ribose							
^{1}H	5.93	4.79	4.51	4.35	4.19		
$^{3}J_{HH}$	6.4						
^{13}C	89.6	76.4	73.3	86.6	68.1		

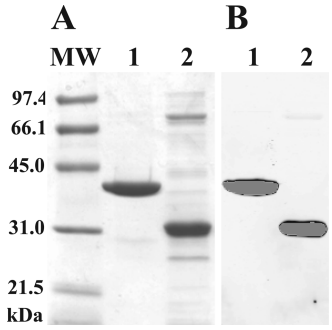

FIGURE 5: SDS−PAGE electrophoresis analysis of purified DmhA and DmhB. The proteins were purified by nickel chromatography. Detection was performed with Coomassie staining (panel A) and anti-histidine tag Western blotting (panel B). Lanes: 1, DmhA; 2, DmhB. DmhA and DmhB were detected at the expected molecular masses of ~40 and 33 kDa, respectively. DmhB dimers that do not totally dissociate despite boiling for 5 min in SDS−PAGE loading buffer prior to SDS−PAGE analysis were also detected by anti-His Western blotting. DmhB is also prone to degradation upon heat treatment, yielding a 25 kDa fragment not present in the original enzyme preparation based on MALDI-MS analysis. MW: molecular mass markers.

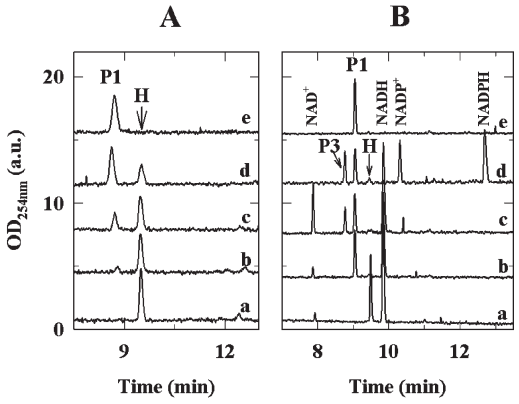

FIGURE 6: CE electrophoregrams showing the conversion of GDP-*manno*-heptose into the new products P1 and P3 upon incubation with DmhA and DmhB. Panel A: Dependency of product formation on the amount of DmhA incubated with GDP-*manno*-heptose. The reaction contained either no DmhA (trace a) or 0.11 (trace b), 0.28 (trace c), 0.55 (trace d), or 5.54 (trace e) pmol of DmhA in a total volume of 10 μL. The reaction also contained 0.15 mM GDP-*manno*-heptose in 200 mM Tris-HCl, pH 9.5, and was incubated for 2 min at 37 °C. Key: H, substrate GDP-*manno*-heptose; P1, reaction product. Panel B: Formation of a new reaction product, P3, upon incubation of GDP-*manno*-heptose with both DmhA and DmhB in the presence of NAD(P)H. Complete reactions (total volume of 10 μL) contained 0.11 pmol of DmhA, 0.11 pmol of DmhB, 0.1 mM GDP-*manno*-heptose, and 0.2 mM NAD(P)H in 200 mM Tris-HCl, pH 8.5, and were incubated for 30 min at 37 °C. Traces: a, no DmhA and no DmhB; b, DmhA only, no DmhB; c, complete reaction with NADH; d, complete reaction with NADPH; e, both enzymes present but no cofactor.

present in control reactions where DmhA was omitted. The amount of product P1 increased with the amount of DmhA for short incubation times so that total conversion of GDP-*manno*-heptose into P1 could readily be obtained (Figure 6A). DmhA exhibited very high levels of activity as significant conversion could be obtained in a very short time even with low amounts of enzyme. Based on the data presented in Figure 6A, the specific activity of DmhA was 667 nmol of GDP-*manno*-heptose converted per nanomole of enzyme per minute.

The addition of NAD(P)$^{+}$ had no impact on the yield or rate of formation of P1 by DmhA (data not shown), suggesting that DmhA had acquired the necessary cofactor during overexpression, as reported for other related dehydratases (*22*−*24*). MS analyses of the supernatant obtained after heat denaturation of purified DmhA demonstrated the presence of a peak at *m*/*z* 662.07 corresponding to NAD^{+} (data not shown). No peak was observed at the *m*/*z* 742 which would be expected for NADP^{+}. Therefore, the purified DmhA harbors NAD^{+}, which explains the fact that no exogenous cofactor is required for catalysis.

Prolonged incubation times led to the appearance of a second peak (called P2 thereafter) with concomitant decrease in the amount of product P1 present (data not shown). No product P2 was observed upon incubation of GDP-*manno*-heptose in the absence of DmhA or upon incubation of DmhA in the absence of GDP-*manno*-heptose (data not shown). This indicated that P2 arises from P1. Ultrafiltration experiments allowed to demonstrate that the formation of product P2 was not enzymatic (Supporting Information Figure 1S). Overall, these data demonstrate that DmhA uses GDP-*manno*-heptose as a substrate and generates rapidly a very unstable product (P1) that transforms nonenzymatically into P2.

DmhB Uses the DmhA Reaction Product as a Substrate. Addition of DmhB to reactions containing DmhA, GDP-*manno*-heptose, and NAD(P)H resulted in the production of a new peak

that migrated upstream of P1 (Figure 6B, product P3), concomitantly with the disappearance of P1 and the formation of $NAD(P)^+$. Formation of this peak was directly proportional to the amount of enzyme present in the reaction and to the reaction time (as long as the substrate was not limiting) and was not observed in the absence of DmhA or of exogenous cofactor. The fact that greater substrate conversion was obtained in the presence of NADPH than with NADH indicates that the preferred cofactor for DmhB is NADPH (Figure 6B) as seen in related reductases (*25*). These data indicate that DmhB uses the reaction product of DmhA as a substrate in an oxidoreduction reaction that oxidizes the NAD(P)H cofactor provided.

MS Analysis of the Reaction Products Generated upon Incubation of DmhA and DmhB with GDP-manno-heptose. The MS pattern of product P1 (generated by DmhA) showed the presence of products at *m*/*z* 616 and at *m*/*z* 638 and 660. The MS/MS patterns of the parent peaks at *m*/*z* 616 (Figure 3B), 638, and 660 (not shown) demonstrated that they were sodium adducts of one another as they yielded similar MS/MS spectra where the main peaks differed in size by 22 mass units (i.e., the mass of the sodium atom) from one spectrum to the other. The product at *m*/*z* 616 exhibited a loss of 18 mass units compared with the original substrate (detected at *m*/*z* 634), which is consistent with the C6 dehydration reaction and formation of the 4-keto-6-deoxy intermediate.

The MS pattern of product P3 (generated by DmhB) showed the presence of a product at *m*/*z* 618 (Figure 3C), which exhibited a gain of 2 mass units compared with P1 (detected at *m*/*z* 616) and a loss of 16 mass units compared with the original substrate (detected at *m*/*z* 634). This is consistent with the C4 reduction of the 4-keto-6-deoxy intermediate produced by DmhA.

The MS/MS fragmentation patterns of the substrate and of P1 and P3 all contained common fragments at *m*/*z* 344, 362, 424, and 442, which correspond to the GDP moiety of the molecule as observed previously (*26*). This indicates that products P1 and P3 arise from the GDP-*manno*-heptose substrate and that DmhA and DmhB did not catalyze any reaction on the GDP moiety, as expected. Importantly, the peak corresponding to the heptose diphosphate fragment of the molecule, which was detected at *m*/*z* 351 in the MS/MS pattern of the original substrate, was shifted by 18 mass units to *m*/*z* 333 in the DmhA product P1 and shifted back to *m*/*z* 335 in the MS/MS spectrum of the DmhB product P3. This is indicating that the dehydration and reduction reactions occurred on the heptose moiety.

In conclusion, these MS data support the hypothesis that DmhA carried out a dehydration reaction on the *manno*-heptose moiety of GDP-*manno*-heptose and that P1 may be the 4-keto-6-deoxy derivative of the substrate, while DmhB carries out the C4 reduction of this 4-keto intermediate and product P3 may be GDP-6-deoxy-*manno*-heptose.

NMR Analysis of the DmhB Reaction Product P3. In contrast to product P1, the DmhB reaction product P3 was stable enough to be purified by anion-exchange chromatography and analyzed by NMR spectroscopy to ascertain its identity. When compared with the original GDP-*manno*-heptose substrate, new signals were observed at 2.07 and 1.67 ppm. DQ-COSY and $^1H-^{13}C$ HSQC analysis indicated these protons resided on the C6 carbon and were coupled to protons on the C5 and C7 positions. The chemical shifts for the C6 methylene signals (H6a, H6b) were also similar with those described before for 6-deoxy-*manno*-heptose that had been extracted directly from *Y. pseudotuberculosis* LPS (*9*, *11*) (Figure 4B, Table 1). In addition, the

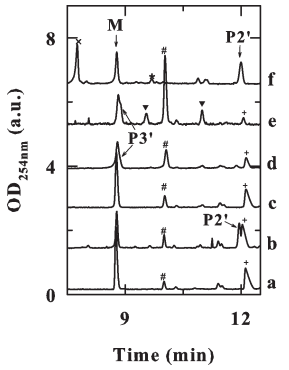

FIGURE 7: CE electrophoregrams showing the conversion of GDP-mannose into the new product P3 upon incubation with DmhA and DmhB. Unless stated otherwise, complete reactions (total volume of 10 μL) contained 22 pmol of DmhA, 7 pmol of DmhB, 0.2 mM GDP-mannose, and 0.2 mM NADPH in 200 mM Tris-HCl, pH 8.5, and were incubated overnight at 37 °C. Traces: a, no enzymes; b, DmhA only, no DmhB; c, DmhB only; d, complete reaction; e, reaction done with 22 pmol of DmhB and 0.1 mM GDP-mannose and incubated for 20 h; f, complete reaction performed with NADH instead of NADPH. Key: M, substrate GDP-mannose; P2′, degradation product arising from the labile GDP-4-keto-6-deoxymannose produced by DmhA (P2′ further degrades upon lengthy incubation at 37 °C, giving rise to peaks highlighted by black triangles in trace e); P3′, GDP-6-deoxymannose; +, NADPH; #, $NADP^+$; *, NADH; ×, NAD^+.

removal of the hydroxyl from C6 caused the obvious loss of the H6 resonances near 3.99 ppm observed in the original substrate. Correspondingly, H4 from the substrate shifted from 3.76 to 3.50 ppm in P3, consistent with a change in the environment of H4 from removal of the hydroxyl group from C6. The remaining portions of the spectra for P3 were very similar to the substrate, including the coupling patterns around the heptose ring. In particular, large coupling constants were measured between H3−H4 and H4−H5 (Table 1), indicating the C3−C4−C5 configuration of the heptose ring appears to be unchanged upon formation of P3. In addition, an NOE between H4 and H6a,b could be identified in two-dimensional ^1H ROESY spectra indicating the configuration of the heptose ring appeared to be the same in the P3 product as the starting GDP-*manno*-heptose substrate.

DmhA Also Uses GDP-mannose as a Substrate. To test whether DmhA is specific for the GDP-*manno*-heptose substrate, its ability to use a related sugar nucleotide from the hexose series, GDP-mannose, was investigated. This reaction was anticipated to produce a GDP-4-keto-6-deoxy-mannose intermediate (thereafter called P1′) that should migrate upstream of GDP-mannose. This hypothesis was verified by using a known GDP-mannose C6 dehydratase, HP0044 (*25*) (data not shown). In contrast, when GDP-mannose was incubated with large amounts of DmhA for long periods of time, the formation of a novel product, P2′, migrating downstream of GDP-mannose was observed on CE (Figure 7). This product was not present in control reactions where DmhA was omitted. Also, increasing the amount of DmhA and the incubation time led to increased conversion of GDP-mannose into P2′. These data demonstrate that DmhA is able to use GDP-mannose as a substrate, although with lower efficiency than its heptose counterpart. Based on CE coinjection analysis, P2′ appeared to be the same species as P2 that was obtained with GDP-*manno*-heptose (data not shown). MS analysis indicated that P2′ corresponds to the GDP portion of the DmhA reaction product as the largest ion detected was at

Table 2: Kinetic Parameters for Catalysis of GDP-*manno*-heptose and GDP-mannose by DmhA

substrate	K_m (mM)	V_{max} (pmol min^{-1})	enzyme (pmol)	k_{cat} (min^{-1})	k_{cat}/K_m (min^{-1} mM^{-1})
GDP-*manno*-heptose	0.23 ± 0.02	240 ± 30	0.2	1100 ± 140	4700 ± 140
GDP-mannose	0.32 ± 0.03	2.7 ± 0.4	11.1	0.25 ± 0.03	0.78 ± 0.06

m/*z* 442 (data not shown). Attempts at detecting the P1′ product by MS have been unsuccessful, probably because of its low abundance and labile character. This is consistent with the fact that 4-keto intermediates are notoriously unstable (*27*, *28*).

DmhB Can Also Use the Labile GDP-4-keto-6-deoxy-mannose Formed by DmhA as a Substrate. As mentioned above, incubation of DmhA with GDP-mannose leads to the formation of P2′, which probably arises from degradation of a labile GDP-4-keto-6-deoxymannose produced by DmhA. When DmhB was added to the DmhA/GDP-mannose reaction in the presence of NADPH, the formation of the degradation product P2′ was not observed, but a new product was observed as a right shoulder on the GDP-mannose peak (Figure 7, peak P3′, trace d). Formation of this product could be enhanced via increasing the DmhB/GDP-mannose ratio, and increasing the incubation time (trace e). Coinjection of this product with GDP-mannose demonstrated that this product is indeed distinct from GDP-mannose (data not shown). Overall, formation of P3′ was poorly efficient and exacerbated the preference of DmhB for its NADPH cofactor, as no new product was observed in the presence of NADH (trace f) or in the absence of cofactor (data not shown). Also, no new product was formed upon incubation of DmhB with GDP-mannose in the absence of DmhA (trace c), thereby confirming that the activity of DmhB is dependent on the formation of the 4-keto intermediate by DmhA.

MS analysis performed on a complete reaction revealed the existence of a peak at *m*/*z* 588 (full product is 589), i.e., 16 mass units smaller than GDP-mannose. The MS/MS fragmentation pattern of this peak contained a fragment unique to the DmhB reaction that was detected at *m*/*z* 305 (data not shown). This was 16 mass units smaller than the hexose ring peak that was detected at *m*/*z* 321 in the parent substrate. The MS/MS pattern also contained peaks corresponding to the unaffected GDP moiety (at *m*/*z* 273, 344, 362, 424, and 442; data not shown). These data are consistent with the occurrence of a C6 dehydration followed by a C4 reduction reaction on the mannose ring, as observed for the heptose substrate.

Physicokinetic Parameters for the DmhA and DmhB Activities. As determined using GDP-*manno*-heptose as a substrate, the activity of DmhA was optimal at pH 9−9.5 and at 37 °C, and that of DmhB was optimal at pH 8.5−9 and 30 °C (data not shown).

K_m and V_{max} determinations for the formation of P1 by DmhA were performed under optimal conditions of 37 °C, pH 9.5, and short reaction times (2 min) to ensure linearity of product formation over time, absence of P2 formation, and to limit product conversion to < 10% of the total substrate present to allow for Michaelis−Menten analysis. As summarized in Table 2, the K_m for GDP-*manno*-heptose was 0.23 mM, which indicates relatively strong affinity of DmhA for its substrate. The k_{cat} and turnover value k_{cat}/K_m were very high, consistent with the fast disappearance of the substrate peak observed on CE even with picomole amounts of enzyme and short reaction times.

As seen with the heptose substrate, DmhA was significantly more active at basic pH than neutral pH when using GDP-mannose as a substrate (data not shown). The K_m and V_{max} for catalysis of GDP-mannose by DmhA were also determined under optimal conditions of 37 °C and pH 9.5, although the incubation times and amounts of DmhA enzyme used were much higher than for GDP-*manno*-heptose to allow significant (5−10%) conversion of GDP-mannose. The K_m for GDP-mannose was 0.32 mM, which is of the same order of magnitude as for the GDP-*manno*-heptose substrate (Table 2). However, the k_{cat} and k_{cat}/K_m were very low, consistent with the slow disappearance of the substrate peak observed on CE even with high enzyme/substrate ratios and long reaction times. These data indicate that although DmhA can use GDP-mannose as a substrate and has equally high affinity for GDP-mannose as for GDP-*manno*-heptose, it is 4500-fold (based on k_{cat}) to 6000-fold (based on k_{cat}/K_m) more efficient at catalyzing the conversion of GDP-*manno*-heptose into P1 than at catalyzing dehydration of GDP-mannose. This suggests that its physiological substrate is GDP-*manno*-heptose rather than GDP-mannose.

The 4-keto intermediates generated by DmhA with either the heptose or the hexose substrates were too unstable to allow kinetic analysis of DmhB.

DISCUSSION

To the best of our knowledge, DmhA and DmhB are the first GDP-*manno*-heptose C6 dehydratase and GDP-4-keto-6-deoxy-*manno*-heptose C4 reductase characterized so far, and this report is the first biochemical analysis of the complete 6-deoxyheptose biosynthesis pathway. The characterization of the first UDP-GlcNAc C6 dehydratase FlaA1 less than 10 years ago (*23*) opened the way to the biochemical characterization of the complete LPS and protein glycosylation biosynthesis pathways in a variety of bacterial pathogens (*17*, *24*, *28*−*31*). Likewise, we surmise that the characterization of DmhA and its associated reductase DmhB will have high impact for the biochemical characterization of LPS and capsule biosynthesis pathways as they govern the first dedicated steps for the production of the 6-deoxyheptoses of various configurations that are found in the LPS and/or capsule of several pathogens (*1*−*8*). The determination of the optimal reaction conditions for DmhA and DmhB reported in this study now also opens the possibility for screening for inhibitors with potential therapeutic value. However, the difficulty in obtaining large amounts of substrate might be a limiting factor for such an endeavor. An alternative will be the rational design of inhibitors based on structural data. The structures of DmhA and DmhB are not currently available. This work demonstrates that high yields of very pure DmhA and DmhB can easily be produced to investigate their structure using a crystallographic approach. In combination with a site-directed mutagenesis approach, this will also allow the identification of the structural determinants for heptose versus hexose substrate specificity by examination of the substrate binding sites of DmhA and DmhB and their comparison to known GDP-mannose dehydratases and reductases (*25*, *32*−*36*).

The biochemical characterization of DmhB and complete characterization of its reaction product were important as they can now serve as a reference for the study of related reductases present in other species. This is significant as the reductases do not exhibit quite as high similarities as the dehydratases, which could imply functional differences. For example, the DmhA homologue (WcbK) found in *C. jejuni* strain 81-176 that harbors 6-deoxy-*altro*-heptose in its capsule (*8*, *37*) is 78% identical and 87% similar to the *Y. pseudotuberculosis* DmhA. In contrast, the best hit for the candidate reductase in this strain, WcaG, only exhibits 23% identity and 43% similarity to the *Y. pseudotuberculosis* DmhB. It will be interesting to investigate whether the reductase WcaG is involved in changes in ring configuration, using DmhB and its characterized product as references.

MS analyses support the hypothesis that the reaction product of DmhA (P1) is GDP-4-keto-6-deoxy-*lyxo*-heptose. Although no analysis of product P1 was possible beyond MS due to its extreme lability, the identity of P1 is consistent with the fact that the modified heptose present in the O-antigen of *Y. pseudotuberculosis* is also in the same, unaltered *manno* configuration as that of the substrate. In some cases, C6 dehydration can be accompanied by C5 epimerization (*27*, *28*) or C4/C5 enolization (*22*), resulting in inversion of the ring configuration. However, such a step is unnecessary for the synthesis of the *manno*-heptose present in the O-antigen of *Y. pseudotuberculosis*. Also, modified heptoses of altered configuration are found in the capsule or exopolysaccharide of a variety of *Campylobacter* isolates (*4*, *8*, *37*−*42*). The corresponding gene clusters also encode putative epimerases that could be responsible for the ring configuration change (*37*, *43*). The O-antigen cluster that encodes DmhA and DmhB does not encode for any candidate epimerase that could restore the original configuration (*10*, *44*). All of this suggests that the configuration of the heptose ring is retained during C6 dehydration. The identity of P1 as GDP-4-keto-6-deoxy-*lyxo*-heptose was further supported by MS and NMR analyses of its derivative P3, obtained from catalysis of P1 by DmhB (P3).

It is somewhat surprising that the optimal activity of DmhA is 37 °C since O-antigen production is downregulated at 37 °C (*45*). This suggests that O-antigen regulation in *Y. pseudotuberculosis* might not encompass the biosynthesis of required precursors but rather might concern their assembly and export to the bacterial surface. Also, the basic optimal pH and the slight differences of optimal conditions observed between DmhA and DmhB were unexpected since the optimal pHs are higher than the cytoplasmic pH that the enzymes are exposed to, and both enzymes would be anticipated to function optimally under the same conditions since they belong to the same biochemical pathway.

DmhA and DmhB can perform their activity on both the heptose and the hexose substrates. C6 dehydration and reduction of GDP-mannose is usually associated with the formation of GDP-L-fucose or of GDP-perosamine (*34*, *36*). MS data obtained for the reduced product P3′ are consistent with the formation of either compound, but we could not generate enough material to distinguish between both compounds by NMR. Also, neither fucose nor perosamine have been reported in the surface carbohydrates of *Y. pseudotuberculosis*, but they may be part of protein glycosylation motifs. Importantly though, although DmhA has similar K_m values for GDP-*manno*-heptose and GDP-mannose, and although these K_m are comparable to the K_m of known GDP-mannose (or other sugar nucleotide) C6 dehydratases (*34*, *35*, *46*), the kinetic analysis performed in this study suggests that the yields for such compounds would be extremely small compared with the production of 6-deoxyheptose dedicated to LPS synthesis. Indeed, the k_{cat} of DmhA for GDP-mannose is 5−10-fold smaller than that of the *H. pylori* or human GMD (*33*, *34*). No kinetic analysis of DmhB was possible for the lack of stable substrate, but very limited conversion of the 4-keto-6-deoxy-*manno* intermediate was obtained after lengthy incubation with abundant DmhB, as opposed to the very rapid and complete conversion of the 4-keto-6-deoxy-*manno*-heptose obtained with trace amounts of DmhB. Hence, the physiological substrate for DmhA/DmhB is not GDP-mannose but is indeed GDP-*manno*-heptose, which the enzymes use to generate 6-deoxyheptose for O-antigen synthesis as demonstrated genetically previously (*9*).

Several Gram-negative bacteria, including *Y. pseudotuberculosis* and *C. jejuni*, harbor two biosynthetic pathways to generate nucleotide-activated *manno*-heptose (*43*, *47*). One uses ADP-L-glycero-β-D-*manno*-heptose and is, among others, utilized for LPS core synthesis, whereas the other uses GDP-D-*glycero*-α-D-*manno*-heptose (*14*, *48*). The reason for the existence of two pathways is not clear in most cases. If a single form of nucleotide-activated *manno*-heptose was shared between various pathways, it would be difficult for the cell to control the level of activity of potent dehydratases to generate enough dehydrated heptose for O-antigen or capsule synthesis without depleting the intracellular pool of primary heptose and ensure appropriate levels of lipid A-core synthesis which are necessary for membrane stability. The kinetic analysis that shows the extremely high catalytic efficiency of DmhA for conversion of GDP-*manno*-heptose into GDP-4-keto-6-deoxy-*lyxo*-heptose brings some rationale for the existence of both pathways: the high activity of DmhA on the GDP-based precursor should not compromise the stock of ADP-based precursor dedicated to lipid-A core synthesis. The activity of DmhA on ADP-*glycero*-*manno*-heptose was not tested in this study for lack of substrate, but sugar nucleotide C6 dehydratases usually use the nucleotide as a fixed handle while catalysis proceeds on the sugar moiety. Consequently, they are usually very specific and exclusive for a given nucleotide, and no activity would be expected for DmhA with ADP-bound sugars.

Prior genetics studies suggested that DmhA might interact with DmhB to be active *in vivo*, as it was not possible to complement a *dmhA* mutant in the absence of functional DmhB encoded in cis from *dmhA* (*9*). This biochemical study clearly demonstrates that DmhA functions with very high efficiency on its own *in vitro*, in the absence of any DmhB. It is possible that an interaction between DmhA and DmhB is actually needed *in vivo* to allow the completion of deoxy-*manno*-heptose synthesis, not for DmhA activity per se, but rather for channeling of its extremely unstable reaction product (P1) to the reductase DmhB. This would avoid unproductive degradation of P1 into P2. Also, this would be important to prevent DmhA from sequestering available GDP-mannose for which it has high affinity and which might then be lacking from other pathways important for cell survival or virulence. Such a channeling mechanism has also been proposed for related enzymes involved in protein glycosylation biosynthetic pathways (*24*).

In summary, this study is the first characterization of a heptose C6 dehydratase and its associated reductase and opens up many possibilities to decipher the modified heptose biosynthetic pathways that support the production of virulence factors in bacterial pathogens. This work has practical implications as it will allow advances for the development of therapeutic inhibitors, and it will also allow the synthesis of complex modified heptoses in their

nucleotide-activated forms that can then be used in the enzymatic synthesis of carbohydrate epitopes for vaccination purposes. This work also has fundamental significance as it will allow the elucidation of the structural determinants that govern the substrate specificity and segregation of heptose versus hexose C6 dehydratases and associated reductases.

ACKNOWLEDGMENT

We thank Dr. P. Reeves for providing the sequence for DmhA before its release on-line at the onset of this project. We thank Dr. P. Messner (Vienna, Austria) for providing the starter pDONR201 plasmids for GmhA/B/C/D and M. D'Elia (Dr. Brown's laboratory, Mc Master University) for transferring the GmhA/B/C/D genes into the pDEST vectors. We thank V. Soo for cloning HP0044 in the GST-tag vector system. Finally, we thank P. Hopf for assistance with softwares and computer issues and S. Kichler for assistance with Western blotting.

SUPPORTING INFORMATION AVAILABLE

Figure 1S containing data demonstrating that the formation of product P2, that occurs over time after incubation of DmhA and GDP-*manno*-heptose, is nonenzymatic. This material is available free of charge via the Internet at http://pubs.acs.org.

REFERENCES

1. Samuelsson, K., Lindberg, B., and Brubaker, R. R. (1974) Structure of O-specific side chains of lipopolysaccharides from *Yersinia pseudotuberculosis*. *J. Bacteriol. 117*, 1010–1016.
2. Skurnik, M., and Zhang, L. (1996) Molecular genetics and biochemistry of *Yersinia* lipopolysaccharide. *APMIS 104*, 849–872.
3. Komandrova, N. A., Gorshkova, R. P., Isakov, V. V., and Ovodov Iu, S. (1984) Structure of O-specific polysaccharide isolated from the *Yersinia pseudotuberculosis* serotype 1A lipopolysaccharide. *Bioorg. Khim. 10*, 232–237.
4. St. Michael, F., Szymanski, C. M., Li, J., Chan, K. H., Khieu, N. H., Larocque, S., Wakarchuk, W. W., Brisson, J. R., and Monteiro, M. A. (2002) The structures of the lipooligosaccharide and capsule polysaccharide of *Campylobacter jejuni* genome sequenced strain NCTC 11168. *Eur. J. Biochem. 269*, 5119–5136.
5. Knirel, Y. A., Paramonov, N. A., Shashkov, A. S., Kochetkov, N. K., Yarullin, R. G., Farber, S. M., and Efremenko, V. I. (1992) Structure of the polysaccharide chains of *Pseudomonas pseudomallei* lipopolysaccharides. *Carbohydr. Res. 233*, 185–193.
6. Perry, M. B., MacLean, L. L., Schollaardt, T., Bryan, L. E., and Ho, M. (1995) Structural characterization of the lipopolysaccharide O antigens of *Burkholderia pseudomallei*. *Infect. Immun. 63*, 3348–3352.
7. DeShazer, D., Waag, D. M., Fritz, D. L., and Woods, D. E. (2001) Identification of a *Burkholderia mallei* polysaccharide gene cluster by subtractive hybridization and demonstration that the encoded capsule is an essential virulence determinant. *Microb. Pathog. 30*, 253–269.
8. Aspinall, G. O., McDonald, A. G., and Pang, H. (1992) Structures of the O chains from lipopolysaccharides of *Campylobacter jejuni* serotypes O:23 and O:36. *Carbohydr. Res. 231*, 13–30.
9. Ho, N., Kondakova, A. N., Knirel, Y. A., and Creuzenet, C. (2008) The biosynthesis and biological role of 6-deoxyheptose in the lipopolysaccharide O-antigen of *Yersinia pseudotuberculosis*. *Mol. Microbiol. 68*, 424–447.
10. Pacinelli, E., Wang, L., and Reeves, P. R. (2002) Relationship of *Yersinia pseudotuberculosis* O antigens IA, IIA, and IVB: the IIA gene cluster was derived from that of IVB. *Infect. Immun. 70*, 3271–3276.
11. Kondakova, A. N., Ho, N., Bystrova, O. V., Shashkov, A. S., Lindner, B., Creuzenet, C., and Knirel, Y. A. (2008) Structural studies of the O-antigens of *Yersinia pseudotuberculosis* O:2a and mutants thereof with impaired 6-deoxy-D-*manno*-heptose biosynthesis pathway. *Carbohydr. Res. 343*, 1383–1389.
12. Graziani, A., Zamyatina, A., and Kosma, P. (2004) A convenient synthesis of GDP D-*glycero*-alpha-D-*manno*-heptopyranose. *Carbohydr. Res. 339*, 147–1451.
13. Kneidinger, B., Graninger, M., Puchberger, M., Kosma, P., and Messner, P. (2001) Biosynthesis of nucleotide-activated D-*glycero*-D-*manno*-heptose. *J. Biol. Chem. 276*, 20935–20944.
14. Kneidinger, B., Marolda, C., Graninger, M., Zamyatina, A., McArthur, F., Kosma, P., Valvano, M. A., and Messner, P. (2002) Biosynthesis pathway of ADP-L-*glycero*-beta-D-*manno*-heptose in *Escherichia coli*. *J. Bacteriol. 184*, 363–369.
15. Newton, D. T., and Mangroo, D. (1999) Mapping the active site of the *Haemophilus influenzae* methionyl-tRNA formyltransferase: residues important for catalysis and tRNA binding. *Biochem. J. 339* (Part 1), 63–69.
16. Moore, J. T., Uppal, A., Maley, F., and Maley, G. F. (1993) Overcoming inclusion body formation in a high-level expression system. *Protein Expression Purif. 4*, 160–163.
17. Obhi, R. K., and Creuzenet, C. (2005) Biochemical characterization of the *Campylobacter jejuni* Cj1294, a novel UDP-4-keto-6-deoxy-GlcNAc aminotransferase that generates UDP-4-amino-4,6-dideoxy-GalNAc. *J. Biol. Chem. 280*, 20902–20908.
18. Bax, A., and Davis, D. G. (1985) MLEV-17-based two-dimensional homonuclear magnetization transfer spectroscopy. *J. Magn. Reson. 65*, 355–360.
19. Piantini, U., Sorensen, O. W., and Ernst, R. R. (1982) Multiple quantum filters for elicidating NMR coupling networks. *J. Am. Chem. Soc. 104*, 6800–6801.
20. Kay, L. E., Keifer, P., and Saarinen, T. (1992) Pure absorption gradient enhanced heteronuclear single quantum correlation spectroscopy with improved sensitivity. *J. Am. Chem. Soc. 114*, 10663–10665.
21. John, B. K., Plant, D., and Hurd, R. E. (1992) Improved proton-detected heteronuclear correlation using gradient-enhanced z and zz filters. *J. Magn. Reson. A101*, 113–117.
22. Ishiyama, N., Creuzenet, C., Miller, W. L., Demendi, M., Anderson, E. M., Harauz, G., Lam, J. S., and Berghuis, A. M. (2006) Structural studies of FlaA1 from *Helicobacter pylori* reveal the mechanism for inverting 4,6-dehydratase activity. *J. Biol. Chem. 281*, 24489–24495.
23. Creuzenet, C., Schur, M. J., Li, J., Wakarchuk, W. W., and Lam, J. S. (2000) FlaA1, a new bifunctional UDP-GlcNAc C_6 Dehydratase/C_4 reductase from *Helicobacter pylori*. *J. Biol. Chem. 275*, 34873–34880.
24. Creuzenet, C. (2004) Characterization of CJ1293, a new UDP-GlcNAc C6 dehydratase from *Campylobacter jejuni*. *FEBS Lett. 559*, 136–140.
25. Wu, B., Zhang, Y., and Wang, P. G. (2001) Identification and characterization of GDP-d-mannose 4,6-dehydratase and GDP-l-fucose snthetase in a GDP-l-fucose biosynthetic gene cluster from *Helicobacter pylori*. *Biochem. Biophys. Res. Commun. 285*, 364–371.
26. Ramm, M., Wolfender, J. L., Queiroz, E. F., Hostettmann, K., and Hamburger, M. (2004) Rapid analysis of nucleotide-activated sugars by high-performance liquid chromatography coupled with diode-array detection, electrospray ionization mass spectrometry and nuclear magnetic resonance. *J. Chromatogr. A 1034*, 139–148.
27. McNally, D. J., Schoenhofen, I. C., Mulrooney, E. F., Whitfield, D. M., Vinogradov, E., Lam, J. S., Logan, S. M., and Brisson, J. R. (2006) Identification of labile UDP-ketosugars in *Helicobacter pylori, Campylobacter jejuni* and *Pseudomonas aeruginosa*: key metabolites used to make glycan virulence factors. *ChemBioChem 7*, 1865–1868.
28. Schoenhofen, I. C., McNally, D. J., Vinogradov, E., Whitfield, D., Young, N. M., Dick, S., Wakarchuk, W. W., Brisson, J. R., and Logan, S. M. (2006) Functional characterization of dehydratase/aminotransferase pairs from *Helicobacter* and *Campylobacter*: enzymes distinguishing the pseudaminic acid and bacillosamine biosynthetic pathways. *J. Biol. Chem. 281*, 723–732.
29. Creuzenet, C., and Lam, J. S. (2001) Topological and functional characterization of WbpM, an inner membrane UDP-GlcNAc C_6 dehydratase essential for lipopolysaccharide biosynthesis in *Pseudomonas aeruginosa*. *Mol. Microbiol. 41*, 1295–1310.
30. Schoenhofen, I. C., McNally, D. J., Brisson, J. R., and Logan, S. M. (2006) Elucidation of the CMP-pseudaminic acid pathway in *Helicobacter pylori*: synthesis from UDP-N-acetylglucosamine by a single enzymatic reaction. *Glycobiology 16*, 8C–14C.
31. Vijayakumar, S., Merkx-Jacques, A., Ratnayake, D., Gryski, I., Obhi, R. K., Houle, S., Dozois, C., and Creuzenet, C. (2006) Cj1121c, a novel UDP-4-keto-6-deoxy-GlcNAc C4 aminotransferase essential for protein glycosylation and virulence in *Campylobacter jejuni*. *J. Biol. Chem. 281*, 27733–27743.
32. Bisso, A., Sturla, L., Zanardi, D., De Flora, A., and Tonetti, M. (1999) Structural and enzymatic characterization of human recombinant GDP-D-mannose-4,6-dehydratase. *FEBS Lett. 456*, 370–374.
33. Sullivan, F. X., Kumar, R., Kriz, R., Stahl, M., Xu, G. Y., Rouse, J., Chang, X. J., Boodhoo, A., Potvin, B., and Cumming, D. A. (1998) Molecular cloning of human GDP-mannose 4,6-dehydratase and reconstitution of GDP-fucose biosynthesis in vitro. *J. Biol. Chem. 273*, 8193–8202.

34. Wu, B., Zhang, Y., and Wang, P. G. (2001) Identification and characterization of GDP-D-mannose 4,6-dehydratase and GDP-l-fucose synthetase in a GDP-l-fucose biosynthetic gene cluster from *Helicobacter pylori*. *Biochem. Biophys. Res. Commun. 285*, 364–371.
35. Sturla, L., Bisso, A., Zanardi, D., Benatti, U., De Flora, A., and Tonetti, M. (1997) Expression, purification and characterization of GDP-D-mannose 4,6-dehydratase from *Escherichia coli*. *FEBS Lett. 412*, 126–130.
36. Albermann, C., and Piepersberg, W. (2001) Expression and identification of the RfbE protein from *Vibrio cholerae* O1 and its use for the enzymatic synthesis of GDP-D-perosamine. *Glycobiology 11*, 655–661.
37. Karlyshev, A. V., Champion, O. L., Churcher, C., Brisson, J. R., Jarrell, H. C., Gilbert, M., Brochu, D., St. Michael, F., Li, J., Wakarchuk, W. W., Goodhead, I., Sanders, M., Stevens, K., White, B., Parkhill, J., Wren, B. W., and Szymanski, C. M. (2005) Analysis of *Campylobacter jejuni* capsular loci reveals multiple mechanisms for the generation of structural diversity and the ability to form complex heptoses. *Mol. Microbiol. 55*, 90–103.
38. Aspinall, G. O., McDonald, A. G., Pang, H., Kurjanczyk, L. A., and Penner, J. L. (1993) An antigenic polysaccharide from *Campylobacter coli* serotype O:30. Structure of a teichoic acid-like antigenic polysaccharide associated with the lipopolysaccharide. *J. Biol. Chem. 268*, 18321–18329.
39. Aspinall, G. O., McDonald, A. G., Pang, H., Kurjanczyk, L. A., and Penner, J. L. (1993) Lipopolysaccharide of *Campylobacter coli* serotype O:30. Fractionation and structure of liberated core oligosaccharide. *J. Biol. Chem. 268*, 6263–6268.
40. Aspinall, G. O., Monteiro, M. A., and Pang, H. (1995) Lipo-oligosaccharide of the *Campylobacter lari* type strain ATCC 35221. Structure of the liberated oligosaccharide and an associated extracellular polysaccharide. *Carbohydr. Res. 279*, 245–264.
41. Hanniffy, O. M., Shashkov, A. S., Moran, A. P., Prendergast, M. M., Senchenkova, S. N., Knirel, Y. A., and Savage, A. V. (1999) Chemical structure of a polysaccharide from *Campylobacter jejuni* 176.83 (serotype O:41) containing only furanose sugars. *Carbohydr. Res. 319*, 124–132.
42. Chen, Y. H., Poly, F., Pakulski, Z., Guerry, P., and Monteiro, M. A. (2008) The chemical structure and genetic locus of *Campylobacter jejuni* CG8486 (serotype HS:4) capsular polysaccharide: the identification of 6-deoxy-D-*ido*-heptopyranose. *Carbohydr. Res. 343*, 1034–1040.
43. Parkhill, J., Wren, B. W., Mungall, K., Ketley, J. M., Churcher, C., Basham, D., Chillingworth, T., Davies, R. M., Feltwell, T., Holroyd, S., Jagels, K., Karlyshev, A. V., Moule, S., Pallen, M. J., Penn, C. W., Quail, M. A., Rajandream, M. A., Rutherford, K. M., van Vliet, A. H., Whitehead, S., and Barrell, B. G. (2000) The genome sequence of the food-borne pathogen *Campylobacter jejuni* reveals hypervariable sequences. *Nature 403*, 665–668.
44. Skurnik, M., Venho, R., Toivanen, P., and al-Hendy, A. (1995) A novel locus of *Yersinia enterocolitica* serotype O:3 involved in lipopolysaccharide outer core biosynthesis. *Mol. Microbiol. 17*, 575–594.
45. Straley, S. C., and Perry, R. D. (1995) Environmental modulation of gene expression and pathogenesis in *Yersinia*. *Trends Microbiol. 3*, 310–317.
46. Sullivan, F. X., Kumar, R., Kriz, R., Stahl, M., Xu, G. Y., Rouse, J., Chang, X. J., Boodhoo, A., Potvin, B., and Cumming, D. A. (1998) Molecular cloning of human GDP-mannose 4,6-dehydratase and reconstitution of GDP-fucose biosynthesis in vitro. *J. Biol. Chem. 273*, 8193–8202.
47. Skurnik, M., Peippo, A., and Ervela, E. (2000) Characterization of the O-antigen gene clusters of *Yersinia pseudotuberculosis* and the cryptic O-antigen gene cluster of *Yersinia pestis* shows that the plague bacillus is most closely related to and has evolved from *Y. pseudotuberculosis* serotype O:1b. *Mol. Microbiol. 37*, 316–330.
48. Valvano, M. A., Messner, P., and Kosma, P. (2002) Novel pathways for biosynthesis of nucleotide-activated *glycero-manno*-heptose precursors of bacterial glycoproteins and cell surface polysaccharides. *Microbiology 148*, 1979–1989.